Renewable Energy 147 (2020) 2470–2483

Contents lists available at ScienceDirect

Renewable Energy

journal homepage: www.elsevier.com/locate/renene

Optimal sizing of a wind-energy storage system considering battery life

Ye Liu [a, b], Xiaogang Wu [a, b, *], Jiuyu Du [b, **], Ziyou Song [b], Guoliang Wu [c]

[a] College of Electrical and Electronic Engineering, Harbin University of Science and Technology, Harbin, 150080, China
[b] State Key Laboratory of Automotive Safety and Energy, Tsinghua University, Beijing, 100084, China
[c] Electric Power Research Institute, State Grid Heilongjiang Electric Power Company Ltd, Harbin, 150090, China

ARTICLE INFO

Article history:
Received 23 March 2019
Received in revised form
21 September 2019
Accepted 26 September 2019
Available online 27 September 2019

Keywords:
Battery storage plants
Wind energy
Wind power generation
Dynamic programming(DP)

ABSTRACT

A battery energy storage system (BESS) can smooth the fluctuation of output power for micro-grid by eliminating negative characteristics of uncertainty and intermittent for renewable energy for power generation, especially for wind power. By integrated with lithium battery storage system the utilization and overall energy efficiency can be improved. However, this target could be obtained only if the BESS is optimal matched. For this issue, the degradation of battery capacity has a significant impact on the operating costs of Wind-ESS system. The research focus on the optimal method for components sizing of BESS in Wind-ESS system with independent system operators. We present an operating cost model for the hybrid energy storage system considering capacity fading of lithium battery in the cycle life. For the optimal objective of component sizing, the global optimization method of dynamic programming (DP) is adopted by setting operating costs and capacity degradation as optimal objectives under the constrains of performance for lithium battery and requirement for grid operation. Based on the DP algorithm and capacity degradation of battery model, the optimal output of the wind power is obtained. The rule based method and genetic algorithm are also be used for simulation. The simulation results show that compared with other two optimal approaches, capacity degradation and operation cost of energy storage for wind power generation system are significantly reduced.

1. Introduction

Wind power has rapidly developed as a clean and pollution-free renewable energy source throughout the world in recent years and has therefore received extensive attention in a variety of research areas. According to the International Energy Agency (IEA), by 2020, annual global power generation will reach 1282 TWh, an increase of nearly 371% over that of 2009. By 2030, this number will increase further, reaching an estimated 2182 TWh, almost double the output expected in 2020 [1]. Wind power installation and generation data show that wind power is an increasingly mature industry that is quickly transforming into its own market-based system, successfully competing with heavily subsidized fossil fuel power generation technologies. However, even with the increasing installed capacity of wind power, there remains the uncertainty and intermittent generation of wind energy based wind forecasting errors still certainly exist, often having a substantial impact on the power grid in the surrounding region [2]. Therefore, traditional wind power plants usually estimate their overall output of the next stage by predicting wind output in advance and signing agreements with grid-side companies according to this forecasting data. Unfortunately, given various punishment mechanisms, insufficient output often leads to the loss of the offending power plant, so power plant administrators usually conservatively estimate output, which often results in power plants discarding a large number of wind power, thereby contributing to a substantial waste of resources [3,4].

Regardless of response times and adjustment accuracy, an energy storage system (ESS) is far superior to the traditional thermal power unit. Retrofitting ESS is an effective way to address the large-scale grid connection problem of wind power as it advances wind output via energy storage equipment, thus making up for inaccuracies in wind forecasting. The combined operation of a wind power plant and ESS together facilitates the tracking of wind power output, thereby improving the utilization of wind power and the

* Corresponding author. College of Electrical and Electronic Engineering, Harbin University of Science and Technology, Harbin, 150080, China.
** Corresponding author.
E-mail address: dujiuyu@tsinghua.edu.cn (J. Du).

https://doi.org/10.1016/j.renene.2019.09.123
0960-1481/

stability of the grid when a large-scale wind power plant is connected, thus ensuring the safe operation of the power grid [5–7].

In recent years, ESS plays an essential role in wind power plants, and redundant energy in wind farms can be stored in the ESS to save on operating costs. Scholars from various countries have conducted a number of studies focused on applying a battery energy storage system (BESS) to a wind power plant to perform peak clipping and smooth wind power output. In Ref. [8], with a goal of minimizing the difference between the actual and predicted outputs of wind power plants, Ke et al. proposed three control algorithms to compensate for wind energy errors. Considering the life depreciation of an ESS at different discharge depths (DODs), the three algorithms were compared to yield a relatively small resulting ESS capacity. In Ref. [9], Xiong et al. expressed the uncertainty of wind power output by using a scenario tree model, reducing the computational burden via the Benders decomposition algorithm; in their work, they concluded that the capital investment of an ESS can successfully reduce the daily operating costs of the given power system. In Refs. [10,11], Zhang et al. adopted a dynamic charging and discharging interval aimed at minimizing the deviations between the wind power's annual target output and actual output by optimizing the charge and discharge power of each ESS within all separate charging and discharging intervals in a given year, thereby calculating the sensitivity relationship between energy storage investment and overall income.

In Ref. [12], based on the prediction of wind power error, Luo Fengji et al. considered the non-normal distribution and persistence of prediction errors. They established a penalty function to reduce deviations between wind power output and predicted output; furthermore, they optimized the energy storage capacity with the ultimate goal of achieving maximum overall revenue. In Ref. [13], Bludszuweit et al. generated an empirical probability density function according to the estimated wind fo recast error and the state of charge (SOC) distribution of the corresponding ESS, thereby reducing the capacity of the ESS and achieving cost savings. In Ref. [14], by analyzing the historical operational data of a power plant Kargarian et al. sums up the distribution law of wind power output fluctuations, thereby determining the capacity of the ESS by combining the effects of smoothing and cost. In Ref. [15], Baker et al. proposed a method for determining the optimal energy storage capacity of a given wind power system. Considering the inherent uncertainty in prediction errors, they modeled wind prediction error as a random variable adhering to a normal distribution; from this, they developed a two-stage model predictive control (MPC) to derive the optimal storage capacity. The above related research primarily used ESS to compensate for wind forecasting errors, thereby improving wind power utilization and increasing the overall profits earned by using such wind storage systems. However, researchers always according to the charge and discharge amount of the battery and the depth of discharge, the equivalent life of the battery decay is calculated by the equivalent life model. They rarely accurately calculate the lifetime degradation of energy storage system due to irregular charging and discharging behavior during operation. In terms of optimization algorithms, heuristic algorithms are simple and intuitive, but in some cases, it is impossible to guarantee global optimal solutions. However, although the dynamic programming algorithm (DP) has a large amount of computation, it can accurately find the global optimal solution.

Traditional wind power plants usually do not include ESS or only have it with a less capacity. As described above, to improve credibility in terms of their agreement with the power grid, traditional wind power plants often conservatively estimate their output, which leads to a substantial amount of discarded wind power. When a wind power plant is equipped with ESS, its energy management strategies differ based on the differing market mechanisms in each country. Given recent reforms in the electricity market in both Europe and the United States, the power market can be characterized by abundant power generation investments, diversified fuel, a transparent market, and strong anti-interference mechanisms to protect the power grid. The power market is primarily composed of the power generation market, the retail market, and the auxiliary service market [16]; however, a reasonable market-oriented trading mechanism has not yet formed in China, it is difficult for private capital in China to enter the transmission and distribution fields. As such, problems in new energy consumption primarily depend on administrative orders rather than market signals [3]. Based on abovementioned the literature review, this paper focus on the problem of discarded wind power in traditional wind power plants and the feasibility of applying energy storage facilities to compensate for wind output errors. By comparing the three algorithms, a DP method that considers the cost of battery life degradation to optimize ESS sizing. In addition, based on the DP method, the optimal sizing of ESS under different index. This research begins in Section 2 by This research begins in Section 2 by introduce the system structure and working principle, after which the approach to modeling the system operating cost model is proposed. Section 4 investigates the component sizing method for system and section 5 is the simulation results and analysis. The final section will summarize the main finding of this research.

2. System structure and working principle

Fig. 1 shows the structure of the Wind-ESS system. The system consists these components, lithium-ion battery, wind turbines and current converts.

The working mode of the system can be divided as follows:

Mode one: When the wind power plant meets the agreed upon load with the power grid, the ESS and auxiliary peaking service are not required, only the wind power plant provides the required power, as shown in Fig. 2.

Mode two: In mode two, the wind power plant generates excess power and the ESS is able to completely eliminate this excess power. In this case, the power plant preferentially transmits its excess power to the ESS (and the agreed upon load is supplied to the power grid), as shown in Fig. 3.

Mode three: In mode three, the wind power plant generates excess power to the extent that the ESS cannot absorb this excess power and the excess power is discarded. In this mode, if the wind power system has a separate sales vending retailer, the discarded wind power may be purchased at a lower price, thereby reducing operating costs, as shown in Fig. 4.

Mode four: As shown in Fig. 5, when the power generated by the wind power plant is not sufficient to meet the contractually required load with the power grid, but the system prioritizes the ESS to transmit its stored power to the grid.

Mode five: In mode five, both wind power plant and ESS are unable to meet the required load with the power grid. In such cases, the power plant must purchase additional active peaking services to compensate for power difference, as shown in Fig. 6.

In support of the above modes of operation, the ESS installed within the wind power plant can reasonably plan its subsequent charging and discharging behavior according to its remaining available capacity during operation. Tuning this planning process is crucial to a power plant, as it would operate in modes two or four.

During operation, the wind power system is limited by the capacity of the ESS, which, depending on whether insufficient or excessive winds occur, leads to an increase in operating costs. To minimize these operating costs, we need to establish an operating

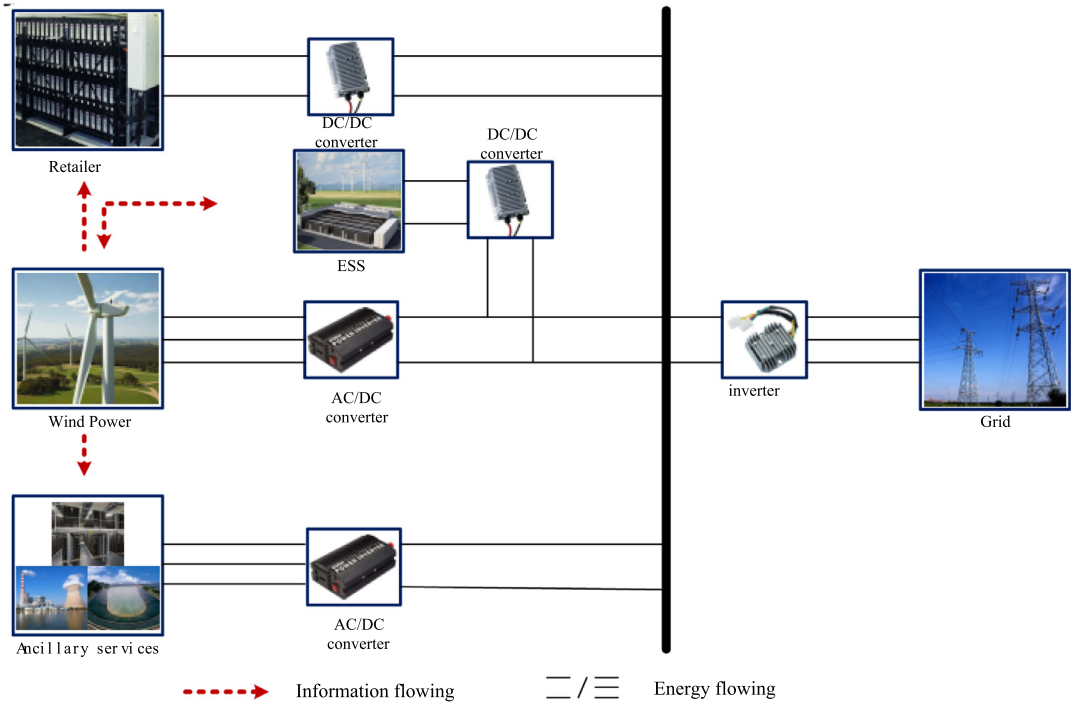

Fig. 1. Wind-ESS system structure.

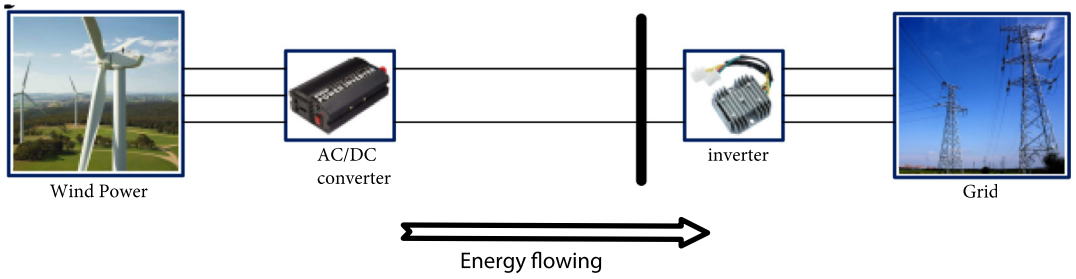

Fig. 2. Wind power system working in mode one.

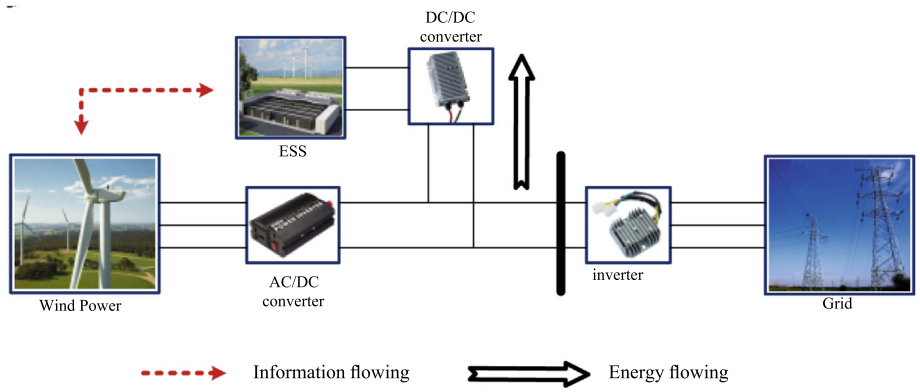

Fig. 3. Wind power system working in mode two.

cost model to facilitate the proper capacity planning of the ESS. The demand of the micro-grid system requires its ESS to have high power density, high energy density, and a fast response time. Combining these required characteristics and changes in future energy storage costs, battery energy storage systems are rapidly becoming the primary energy storage devices in future micro-grid systems; in addition to battery energy storage systems, solutions are also incorporating flywheel energy storage systems, compressed-air energy storage, hydraulic energy storage, etc. [17,18].

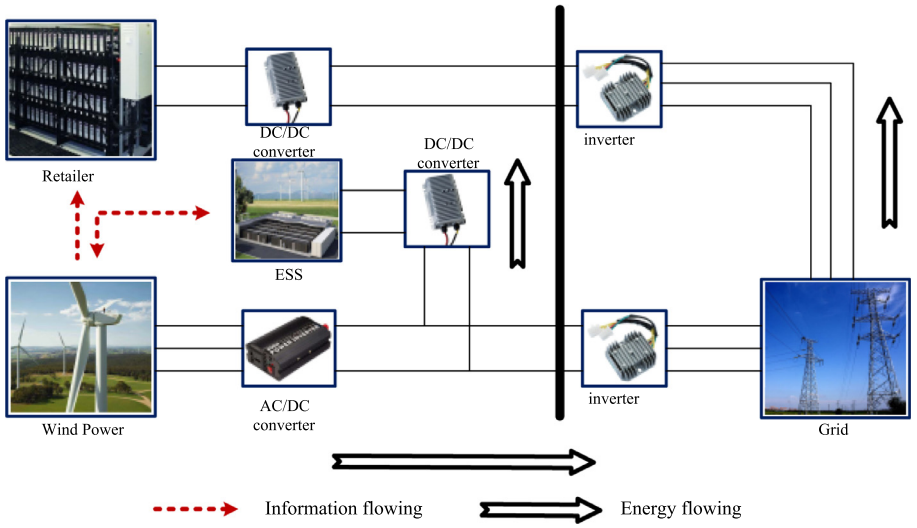

Fig. 4. Wind power system working in mode three.

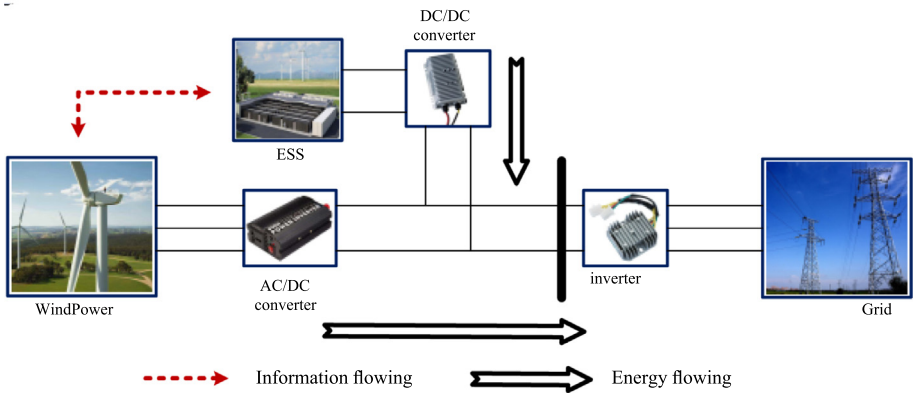

Fig. 5. Wind power system working in mode four.

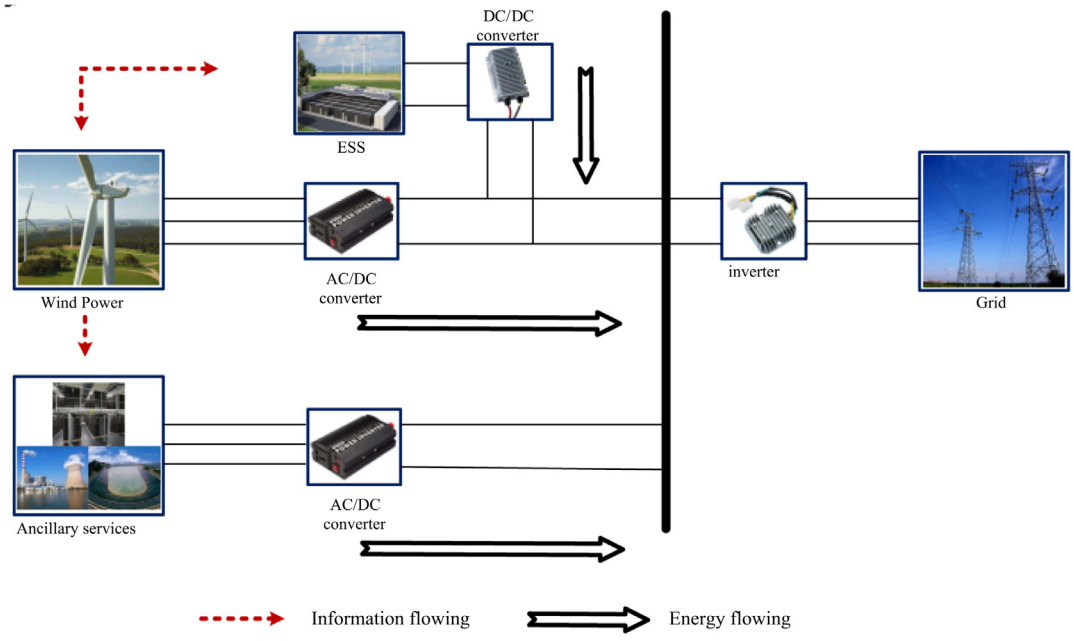

Fig. 6. Wind power system working in mode five.

3. Operating cost model

In order to maximize the operational benefit of the wind power plant, the output of the Wind-ESS system is optimized. By comparing the operating costs saved based on different sizing of ESS, the optimal ESS sizing in wind power plant is obtained.

3.1. Construction of system operating cost model

In order to obtain the optimal sizing of ESS in a wind power plant and minimize the system cost, the objective function is defined as follows:

$$u_n = \sum_{t=1}^{t_{\max}} u_1(t) + u_2(t) + u_3(t) + u_4(t) \tag{1}$$

Here, the operating cost include the cost of discarding generated wind power (u_1), the cost of using an auxiliary peaking service (u_2), the operating cost of BESS (u_3), and the initial investment of ESS (u_4).

3.1.1. Cost model for discarded wind energy

When the output of the wind power plant is greater than the reference load and the state of charge (SOC) of the BESS is more than 90%, the system must discard the excess wind power at a cost, the cost model for discarded wind energy as follows:

$$u_1(t) = \sum_{d=1}^{D} \sum_{t=1}^{24} C_{\mathrm{dw}} P_{\mathrm{dw}}(t) \tag{2}$$

Here, C_{dw} represents the discarded wind energy cost and $P_{\mathrm{dw}}(t)$ is the discarded wind power volume per hours t.

3.1.2. Cost model for auxiliary peaking service

The peaking units in the power system are generally divided into thermal power units and hydropower units. The auxiliary peaking service cost as follows:

$$u_2(t) = \sum_{d=1}^{D} \sum_{t=1}^{24} C_{\mathrm{plo}} P_{\mathrm{plo}}(t) \tag{3}$$

Here, C_{plo} represents the discarded wind energy penalty, which is assumed to be the unit power generation cost of the wind power plant and $P_{\mathrm{plo}}(t)$ is the peaking service power in t-th hour.

3.1.3. Cost model for the ESS

The cost of the energy storage battery includes the cost of battery degradation and the average daily cost-sharing associated with the initial purchase of the batteries. Among them, the degradation cost of the batteries is the operating cost due to irregular charging and discharging while operating the system. At present, the research on the cycle life of LiFePO4 battery mainly focuses on the degradation mechanism, but the mechanism model is more complex, the parameters are more, the calculation amount is large, and it is not easy to realize in engineering. At the same time, the mechanism model may not accurately reflect the battery life attenuation under the complex degradation mechanism of multi-factor coupling. Compared with the mechanism model, the semi-empirical model has less parameters and less computation, so it is easier to be applied in engineering practice [19,20]. After conducting a number of experimental studies on the degradation process of $LiFePO_4$ cells, in Ref. [21], Wang et al. proposed a semi-empirical model for estimating battery capacity degradation as follows:

$$Q_{\mathrm{loss}} = A_0 e^{-\left(\frac{E_a + B \cdot C\_Rate}{RT_{\mathrm{bat}}}\right)} (A_h)^z \tag{4}$$

Here, Q_{loss} represents battery capacity degradation, E_{a} is the activation energy (J/mol), R is the ideal gas constant, C_Rate is the absolute value of the battery charge and discharge current rate, A_{h} is the Ah-throughput, A_0 is the pre-exponential coefficient, z is a second undetermined coefficient, B is a third undetermined coefficient, and T_{bat} is the temperature of the battery in Kelvin. This model is based on the Arrhenius degradation model and considers the effects of different charge/discharge rates and temperature.

Equation (4) can be rearranged as follows:

$$A_h = \left(Q_{\mathrm{loss}} e^{\frac{E_a + B \cdot C\_Rate}{RT_{\mathrm{bat}}}} \Big/ A_0 \right)^{\frac{1}{z}} \tag{5}$$

Next, finding the derivative of A_{h} in Equation (5) yields the following:

$$\dot{Q}_{\mathrm{loss}} = z A_0 e^{\frac{E_a + B \cdot C\_Rate}{RT_{\mathrm{bat}}}} \Big/ (A_h)^{z-1} \tag{6}$$

Combining Equations (5) and (6) over one time step from t to t+1 yields the following:

$$Q_{\mathrm{loss},t+1} - Q_{\mathrm{loss},t} = \Delta A_h z A_0^{\frac{1}{z}} e^{-\left(\frac{E_a + B \cdot C\_Rate}{zRT_{\mathrm{bat}}}\right)} Q_{\mathrm{loss},t}^{\frac{z-1}{z}} \tag{7}$$

Here, $Q_{loss,t+1}$ and $Q_{loss,t}$ are the degradation of the battery from time t to time t+1, respectively, while $\triangle A_{\mathrm{h}}$ is the accumulated ampere-hour throughput of the battery during the same time period, which is determined as follows:

$$\Delta A_h = \int_t^{t+1} |I_{\mathrm{bat}}| dt \tag{8}$$

In Ref. [22], Song et al. calibrated the parameters in Equation (4) with the values shown in Table 1.

Given the above, the operating costs of the battery can be represented as follows:

$$u_3(t) = price_{\mathrm{bat}} \cdot C_{\mathrm{bat}} \cdot V_{\mathrm{bat\_cell}} \cdot \left(2.637 * 10^{-3} * |I_{\mathrm{bat}}(t)| \cdot e^{-\frac{15162 - 1516C\_rate(t)}{2041.52}} \cdot Q_{\mathrm{loss}}(t-1)^{-0.2136}\right) \tag{9}$$

Here, C_{bat} represents the total capacity (Wh) of the ESS and $price_{\mathrm{bat}}$ is the price of the battery (RMB/kWh). Using Equation (9), the estimated battery price in 2020 is 1.0 RMB/Wh. This paper mainly focuses on the performance of the energy storage system under the system power requirement, the accuracy of the dynamic response of the system is not very high, so choosing the battery Rint model can ensure the accuracy of the model in a long time scale, reduce the complexity of the model and the amount of simulation calculation. The Rint model, also known as the internal resistance model, is a relatively simple model designed by the National Laboratory of Idaho. Including battery ideal voltage source U_{oc} and battery internal resistance R_{o}. In addition, I_{bat} is the battery charge and

Table 1
LiFePO4 battery degradation model calibration parameters corresponding to Equation (4).

Parameter (unit)	Value
A_0	0.0032
B	−1516
Z	0.824
E_a (J/mol)	15162
R (J/(mol·K))	8.314
T(K)	298

discharge current according to the following battery Rint model. The battery Rint model is shown in Fig. 7.

$$I_{bat}(t) = \frac{V_{bat} - \sqrt{V_{bat}^2 - 4R_{bat}P_{bat}(t)}}{2R_{bat}} \tag{10}$$

Here, R_{bat} represents the charge and discharge internal resistance of the battery, which Song et al. obtained via experiments [22], with specific data shown in Fig. 8.

In this study, without considering the cost of land, the operating cycle of the ESS was set to 10 years [23]. Thus, the equalization cost of the ESS is then described as follows:

$$u_4(t) = \frac{price_{bat} \cdot C_{bat} \cdot V_{bat\_cell} \cdot t}{3650*24} \tag{11}$$

Here, t represents the system operating time in hours.

3.2. Optimization objectives and constraints

The difference between the predicted power and the actual power of the given wind power plant is defined as demand power P_{demand}. When this demand power is greater than zero, the ESS must be discharged, and vice versa. As an optimization problem, the choice of its optimization step directly affects the size of the optimal result. For a wind power plant, wind power is a volatile source of electricity; therefore, short-term wind power prediction techniques covering one to 72 h are used in power system planning to establish agreements, dispatch energy, and trade power within certain power markets. Medium-term forecasting is used to plan the maintenance and energy storage operations of a wind power plant, and the reasonable continuous discharge time for energy storage and renewable energy cooperation should be several hours [24]. Therefore, this paper set an optimization step size to 1 h [25].

When using the above operating cost model as an optimization function, the corresponding constraints are as follows:

① ESS power constraint:

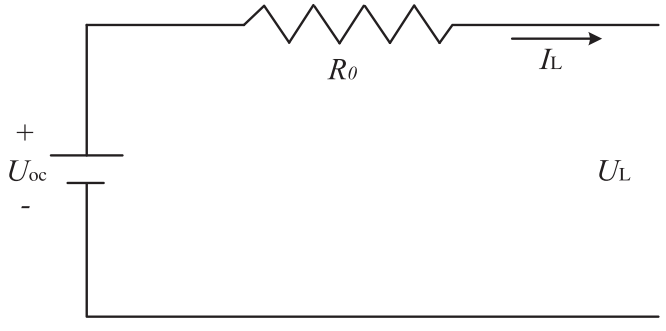

Fig. 7. The Rint model of battery.

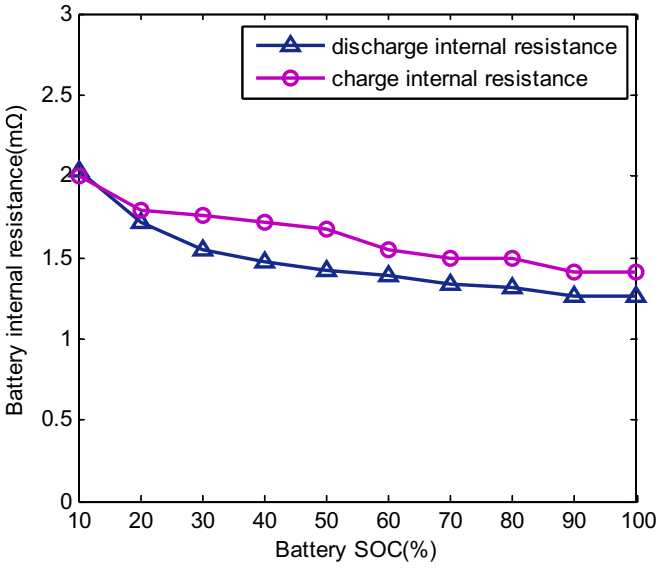

Fig. 8. LiFePO4 battery charge and discharge resistance.

$$0 \le |P_{bat}(t)| \le C_{bat} \tag{12}$$

② ESS capacity constraint:

$$0 \le W_{bat}(t) \le C_{bat} \tag{13}$$

③ Output power constraint

$$0 \le P_{wind}(t) \le C_{wind}/T_s \tag{14}$$

Here, C_{wind} is the nameplate capacity of the given wind power plant.

4. Optimization for ESS matching and energy management strategy

In recent years, scholars from various countries have conducted many research on rule-based energy management algorithms used in ESS instances for new energy power plants [26–28]. In such methods, the optimal solution is obtained using a detailed division of the system state and the working mode of the ESS. Due to limitations of the rules, it is deemed impossible to consider all factors affecting the given system. Therefore, a global optimization cannot be properly achieved. Heuristic algorithms, such as the GA and PSO, are simple and intuitive. However, in some cases, a global optimal solution may not be obtained. To this end, in this paper, by choosing rule-based method (RB), GA and DP, the three methods are simulated and compared.

4.1. Energy management method based on rules

As shown in Fig. 9, a RB in Ref. [26] is referenced for manage the energy flow of Wind-ESS system. The working mode is summarized as follows:

① When $P_{demand}(t) \ge 0$ and the available storage capacity of the ESS can meet P_{demand}, the ESS discharges normally;
② When $P_{demand}(t) \ge 0$ and the available storage capacity of the ESS cannot meet $P_{demand}(t)$, the ESS discharges to its

minimum power level and calculates the peaking cost of the auxiliary service;

③ When $P_{demand}(t) < 0$ and the available charging capacity of the ESS can meet P_{demand}, the ESS is normally charged;

④ When $P_{demand}(t) < 0$ and the available charging space of the ESS cannot meet P_{demand}, the ESS is charged to the highest power level and the cost of discarding the generated wind energy is calculated.

4.2. Energy management method based on genetic algorithm

Genetic algorithm (GA) is an intelligent optimization algorithm based on Darwin's theory of survival of the fittest, which simulates the evolution of natural organisms. It has the characteristics of simple design and strong robustness. In this paper, the output power of ESS is regarded as an individual in GA and coded in the form of real matrix, as shown in equation n.

$$J_k = (P_1, P_2, \ldots, P_t, \ldots, P_{tmax}) \tag{15}$$

Here, k is the k-th individual in genetic algorithm, P is the output power of ESS at time t. The fitness function of the algorithm is:

$$F_{fit}(k) = \max(u_n(k)) - u_n(k) \tag{16}$$

Here, u_n(k) is the Wind-ESS system operating cost of the k-th individual. The convergence speed of the algorithm will be slow if the initial population is generated completely randomly. In order to prevent the crossover and mutation operations in the algorithm from destroying the optimal individuals in each generation population, the individuals with high fitness values are directly retained to the next generation without crossover and mutation operations. For the GA method, the parameters selected in this paper are shown in Table 2, and the flow chart of the genetic algorithm used in this paper is shown in Fig. 10.

4.3. Energy management method based on dynamic programming algorithm

Dynamic programming is a mathematical technique for solving sequential decision problems. More specifically, a dynamic programming algorithm can determine the global optimal solution in a reasonable amount of time. Given this, dynamic planning has a good application prospect for the optimization of energy management algorithms in specific operating conditions [29–32].

In this paper, the calculation of DP method is realized by the following steps:

(1) **Identify the division unit:** One hour is selected as the optimization interval.

(2) **Identify the selection status:** The objective situation in which the problem develops in each stage is expressed via different states and satisfy without aftereffect. More specifically, SOC_{bat} is selected as the state variable.

(3) **Determine the decision and state transition equation:** The specific state transition is based on the state of the previous phase and the decision made to obtain the state of this phase. In this present work, the decision variable is charge and discharge amount $P_{bat} \cdot T_s$ (since the optimization step is 1 h, it can be neglected T_s). Given the above, the corresponding state transition equation is as follows:

Table 2
Parameters of GA method.

Parameter	Value
Population size	500
Crossover fraction	0.9
Migration fraction	0.1
Generations	50
Elite count	1

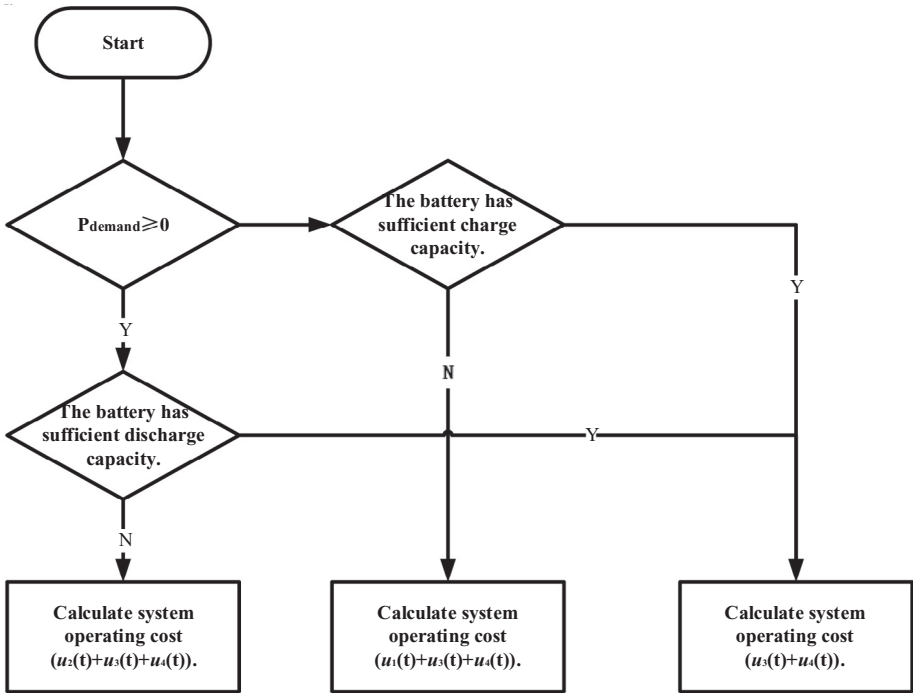

Fig. 9. The flowchart of RB method.

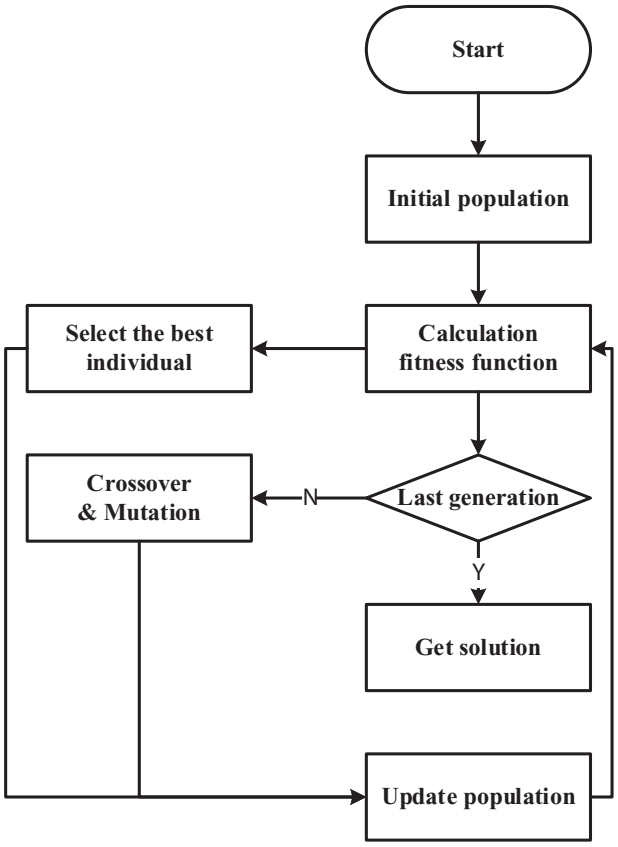

Fig. 10. The flowchart of GA method.

$$SOC_{\mathrm{bat}}(t) = SOC_{\mathrm{bat}}(t-1) - P_{\mathrm{bat}}(t)/C_{\mathrm{bat}} \tag{17}$$

(4) **Determine the evaluation function:** Combining the objective function with the algorithm, the evaluation function is set as follows:

$$f(u_n) = \min \sum_{t=1}^{t_{\max}} C_{\mathrm{price}}[\phi_t(SOC_{\mathrm{bat}}(t), P_{\mathrm{bat}}(t)) + \varphi_t(SOC_{\mathrm{bat}}(t+1))] \tag{18}$$

Here, Φ represents the operating cost incurred by decision P_{bat} at time t and time t+1, while φ represents the minimum operating cost of the system between time t and time t+1.

The two objective functions below use DP method to model the life-saving degradation of the ESS caused by irregular charging and discharging of the ESS during operation:

$$\begin{cases} u_{n1} = \left(\min \sum_{t=1}^{t_{\max}} u_1(t) + u_2(t) + u_4(t) \right) + u_3^{'}(t) \\ u_{n2} = \min \sum_{t=1}^{t_{\max}} u_1(t) + u_2(t) + u_3(t) + u_4(t) \end{cases} \tag{19}$$

More specifically, u_{n1} and u_{n2} are objective functions corresponding to DP method which is labeled DPA and DPB. Note that objective function DPA does not consider battery degradation whereas objective function DPB does. The former achieves global optimality by rationally allocating the charge and discharge power of the ESS, thereby calculating the charge and discharge behavior of the corresponding ESS. Therefore, the resulting battery fading cost is added to the cost of the first three measures. The latter objective function comprehensively considers the four measures and uses dynamic programming to obtain the ideal global optimal solution of the four measures. By comparing the simulation results of these two algorithms, it can be explain the effect irregular charging and discharging has on the life of the ESS.

Since the state of each optimization interval in the objective function is different, the value of the evaluation function is also different, therefore, it is necessary to discuss the required power and the different states that each optimization interval may reach. Here, it can be assume that the remaining energy storage capacity of an optimization interval is represented as $W_{\mathrm{bat}}(t)$.

When $P_{\mathrm{demand}}(t) > 0$, different decisions correspond to the following three cases:

① In this case, $W_{\mathrm{bat}}(t)$-W_{bat} $(t+1) \leq 0$, meaning that the ESS cannot meet the demand power. Given this, $u_1(t)$ and $u_2(t)$ are the objective functions described as follows:

$$\begin{cases} u_1(t) = 0 \\ u_2(t) = P_{\mathrm{demand}}(t) + W_{\mathrm{bat}}(t+1) - W_{\mathrm{bat}}(t) \end{cases} \tag{20}$$

② In this case, $W_{\mathrm{bat}}(t)$-W_{bat} $(t+1) \geq 0$, but the difference here is still less than the required power. In this case, $u_1(t)$ and $u_2(t)$ are the objective functions described as follows:

$$\begin{cases} u_1(t) = W_{\mathrm{bat}}(t+1) - W_{\mathrm{bat}}(t) \\ u_2(t) = P_{\mathrm{demand}}(t) - W_{\mathrm{bat}}(t+1) + W_{\mathrm{bat}}(t) \end{cases} \tag{21}$$

③ In this case, $W_{\mathrm{bat}}(t)$-W_{bat} $(t+1) \geq 0$, and the difference can satisfy the required power needed. In this case, $u_1(t)$ and $u_2(t)$ are the objective functions described as follows:

$$\begin{cases} u_1(t) = W_{\mathrm{bat}}(t+1) - W_{\mathrm{bat}}(t) - P_{\mathrm{demand}}(t) \\ u_2(t) = 0 \end{cases} \tag{22}$$

When $P_{\mathrm{demand}}(t) < 0$, different decisions again correspond to three different situations as follows:

① In this case, $W_{\mathrm{bat}}(t)$-W_{bat} $(t+1) \geq 0$, meaning that the ESS emits a certain amount of electricity, and the actual output of the wind power plant is delivered to the power grid instead of used to charge the ESS battery. In this case, $u_1(t)$ and $u_2(t)$ are objective functions described as follows:

$$\begin{cases} u_1(t) = W_{\mathrm{bat}}(t+1) - W_{\mathrm{bat}}(t) \\ u_2(t) = 0 \end{cases} \tag{23}$$

② In this case, $W_{\mathrm{bat}}(t)$-W_{bat} $(t+1) \leq 0$, and the difference in energy here can be satisfied via the excess power generation of the wind power plant. In this case, $u_1(t)$ and $u_2(t)$ are objective functions described simply as follows:

$$\begin{cases} u_1(t) = 0 \\ u_2(t) = 0 \end{cases} \tag{24}$$

③ In this case, $W_{\mathrm{bat}}(t)$-W_{bat} $(t+1) \leq 0$, and the difference in energy can again be satisfied via the excess power generation of the wind power plant. In this case, $u_1(t)$ and $u_2(t)$ are objective functions described as follows:

$$\begin{cases} u_1(t) = 0 \\ u_2(t) = P_{\text{demand}}(t) - W_{\text{bat}}(t+1) + W_{\text{bat}}(t) \end{cases} \quad (25)$$

Whenever the objective function changes, the evaluation function between the two fixed states and the state transition equation are invariants. Finally, Fig. 11 shows the schematic diagram of DP method.

5. Simulation results and analysis

A wind power plant with a nameplate capacity of 800 MWh is selected for simulation. From the historical operational data of the selected power plant, as shown in Fig. 12, the weekly wind power output monitoring data in a typical climate is selected, including actual output data and reference load data [33].

It can be observed that the wind power plant discards a substantial amount of wind power for lacking of ESS, which results in a high level of energy waste. Nonetheless, it can be also observe here that the sum of the actual wind power output is slightly higher than the sum of the predicted output, meaning that if a reasonable ESS was added to this wind power plant, it could guarantee that its reference load would be satisfied most of the time.

Both Li et al. [34] and Du et al. [35] have presented analyses and economic comparisons of the efficiency and modes of the existing energy storage equipment connected to the power grid. From their work, BESS is deemed suitable for a variety of distributed systems due to its flexible capacity, power characteristics, and its relatively compact size. Further, a $LiFeFO_4$ battery is widely used in ESS installations given its excellent durability, high energy density, and high monomer voltage. Table 3 lists the battery parameters selected in this study.

Further, the on-grid price of the wind power plant is selected to be 0.56 RMB/kWh and C_{dw} is selected to be 0.65 RMB/kWh [36]. According to the "2025 China Wind Power and Electricity Cost" white paper issued by General Electric (GE) [37], C_{dw} is expected to decrease to 0.34 RMB/kWh, and sets the efficiency of the converter in the system to 95%. In view of the influence of the depth of discharge on battery life, the battery operating range was set to 20%–90% of its SOC [38] and the initial stage and the termination stage SOC of the battery is set to 55%. Considering the diversity of auxiliary peaking services, this paper sets the auxiliary peaking service price to twice the wind power grid price. In summary, four methods are simulated and compared, in which the capacity of the ESS is set to 500 MWh. Given the above, Figs. 12 and 13 show the output power of ESS and the degradation of battery life of four methods.

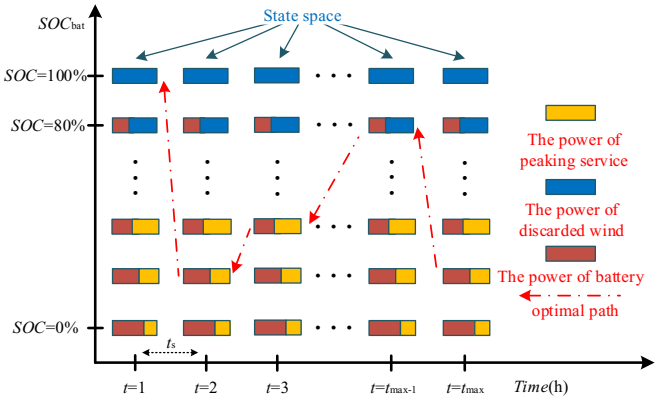

Fig. 11. Schematic diagram of DP method.

As shown in Figs. 13 and 14, charging and discharging power of four methods is compared. It can be observe that the rules-based energy distribution system gives priority to charging the ESS, which leads to the repeated charging and discharging of ESS, thereby accelerating battery degradation. The working mode of GA method is similar to that of RB method, but the output power of ESS is less than that of RB method in some time periods. Due to the limitation of the GA method, it is difficult to obtain the global optimal solution. However, the GA method is still better than the RB method to some extent. After that, the DPA method is compared with the DPB method. Without considering battery degradation, the DPB method pre-charge the ESS to the extent possible across several stages when the required power is greater than zero, whereas the remaining time is reduced as much as possible to reserve available charging capacity. However, this charging phenomenon is only concentrated within a few stages, and the charging rate of the battery is relatively high, thereby accelerating battery life degradation. By contrast, in DPA method, the ESS maintains a constant current charging state in most stages while the charging rate is lower than the former three methods, thereby reducing the degradation of battery life. During the discharge phase, the DPA method is also guaranteed to maintain a constant current discharge under the premise of minimizing extra cost. More specifically, Table 4 compares operating costs and shows ESS degradation when C_{dw} is 0.65 RMB/kWh or 0.34 RMB/kWh.

From Table 4, battery degradation is reduced effectively through the DPA degradation. Based on this method, the ESS decays within one year of the wind storage system going online. Compared to the rules-based results, battery degradation for DPA and DPB was reduced by 0.626% and 0.531%, respectively. In conclusion, compared with the other two methods, DPA under the same conditions can effectively reduce overall operating costs and achieve a noticeable cost savings.

According to above simulation results, Fig. 15 shows the optimal output of the Wind-ESS system based on the DPA method of the battery life degradation for different C_{bat} values.

More specifically, Fig. 15 shows the optimal output power of Wind-ESS system with battery capacity ranging from 100 MWh to 800 MWh. The simulation results indicate that when the optimized output power precedes $P_{\text{demand}} > 0$, the ESS is properly charged to meet the subsequent power requirements by utilizing the portion of the actual output that was higher than the reference load portion. Note that this charging behavior is limited by the capacity of the energy storage and, therefore, it is generally not possible to ensure that all inter-zone wind power output is higher than the reference load. Furthermore, as the capacity of the ESS increases, the range of load requirements that can be satisfied gradually increases. but because of the operational data determined and shown in the graphs, when the ESS has enough power and the actual power output is insufficient (i.e., the reference load is higher than the actual output) or if the energy storage capacity is smaller than the storage capacity, there is no change in the optimized output of wind power, even if it continues to increase energy storage capacity.

When the ESS does not have enough power before the wind power output becomes insufficient, the ESS can only output its residual power. In an ideal situation, the optimized output generated directly by the wind can guarantee the reference load and the total generating capacity of the system is then simultaneously equal to the actual total power generation. To achieve this ideal state, the reference load can be met by the wind power plant itself and the storage system alone, while the excess power can be delivered to the power grid in full; however, since this often requires a storage system with a very large capacity, it is not an optimal choice in terms of initial investment or ongoing operating costs. As such, it is

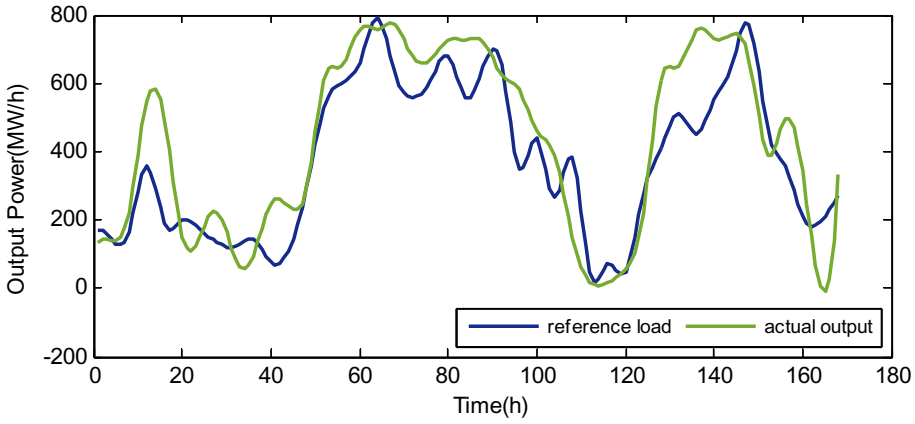

Fig. 12. Reference load and actual output data of the selected wind power plant for our simulation and analysis.

Table 3
LiFePO4 battery cell parameters for our simulation and analysis.

Parameter (unit)	Value
Nominal voltage V_{bat_cell}(V)	3.2
Capacity C_{bat_cell} (A·h)	60
Energy storage (KJ)	831.6
Quality (kg)	2.5
Operating temperature (°C)	−20–45

necessary to weigh the benefits versus the costs of power generation and energy storage to ensure the right energy storage capacity is selected.

Next, Fig. 16 shows the relationship between the calculated ESS capacity (MWh) and the weekly operating cost (RMB) of the wind storage system when C_{dw} is equal to either 0.65 RMB/kWh or 0.34 RMB/kWh.

From Fig. 16, it can observe that with the increase in ESS

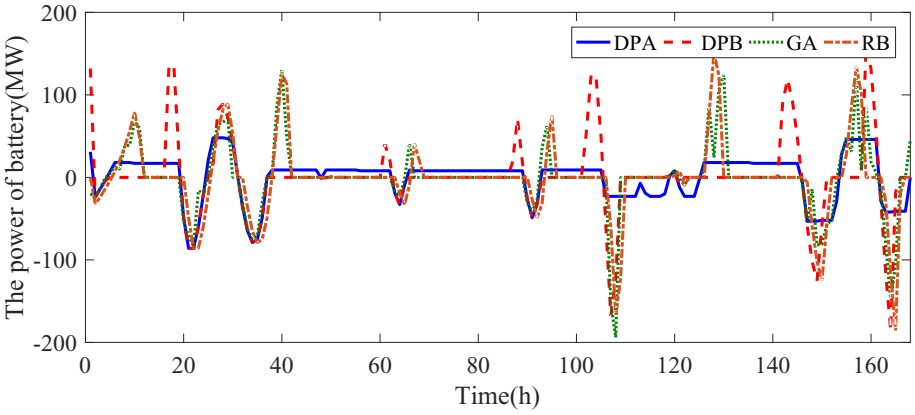

Fig. 13. Output power of the ESS corresponding to four methods.

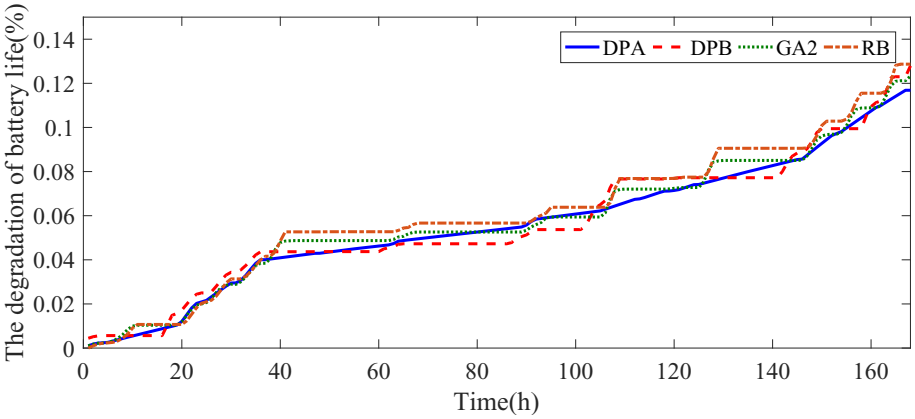

Fig. 14. ESS battery degradation corresponding to four methods.

Table 4
Comparison of operating costs and annual ESS degradation for each of the four methods.

	DPA	DPB	GA	RB
Annual degradation of ESS(%)	0.117	0.127	0.124	0.129
Weekly extra cost ($C_{dw} = 0.65$) (mRMB/year)	10.799	11.025	10.933	11.231
Weekly extra cost ($C_{dw} = 0.34$) (mRMB/year)	7.311	7.537	7.464	7.743

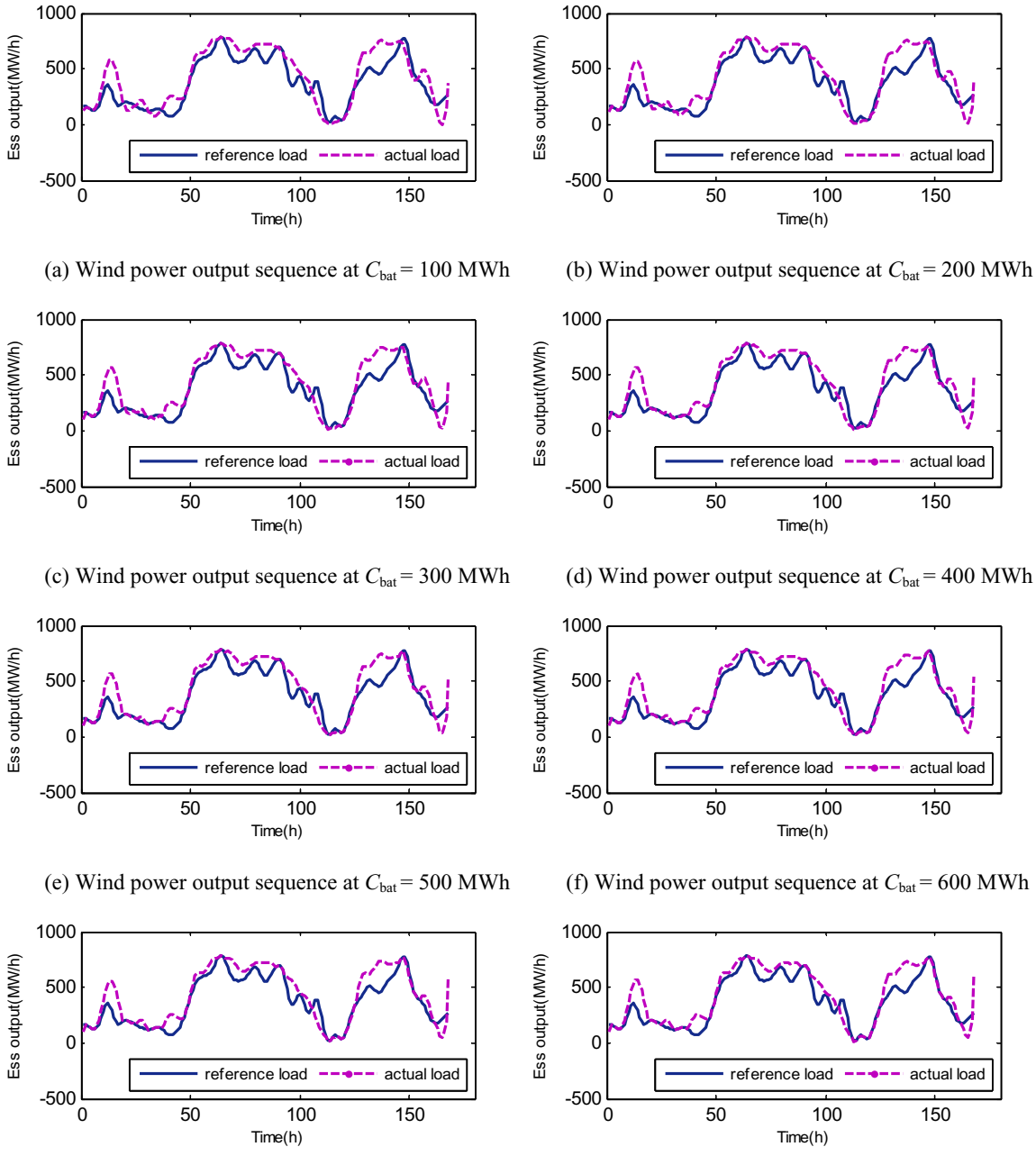

(a) Wind power output sequence at $C_{bat} = 100$ MWh

(b) Wind power output sequence at $C_{bat} = 200$ MWh

(c) Wind power output sequence at $C_{bat} = 300$ MWh

(d) Wind power output sequence at $C_{bat} = 400$ MWh

(e) Wind power output sequence at $C_{bat} = 500$ MWh

(f) Wind power output sequence at $C_{bat} = 600$ MWh

(g) Wind power output sequence at $C_{bat} = 700$ MWh

(h) Wind power output sequence at $C_{bat} = 800$ MWh

Fig. 15. Optimal Wind-ESS system output power for different BESS capacities.

capacity, the operating cost of the wind storage system generally decreased at first, then slightly increased. From the simulation data, we determined that the operating cost of the wind storage system reached its minimum when the capacity of the ESS increased to approximately 945.71 MWh. When the discarded electricity price was reduced to 0.34 RMB/kWh, the optimal capacity of the ESS was 914.29 MWh. Therefore, we conclude here that the operational expenses generated by an increase in ESS capacity are similar; however, when the discarded electricity price was reduced by 47.69%, the optimal capacity was only reduced by 3.32%, showing

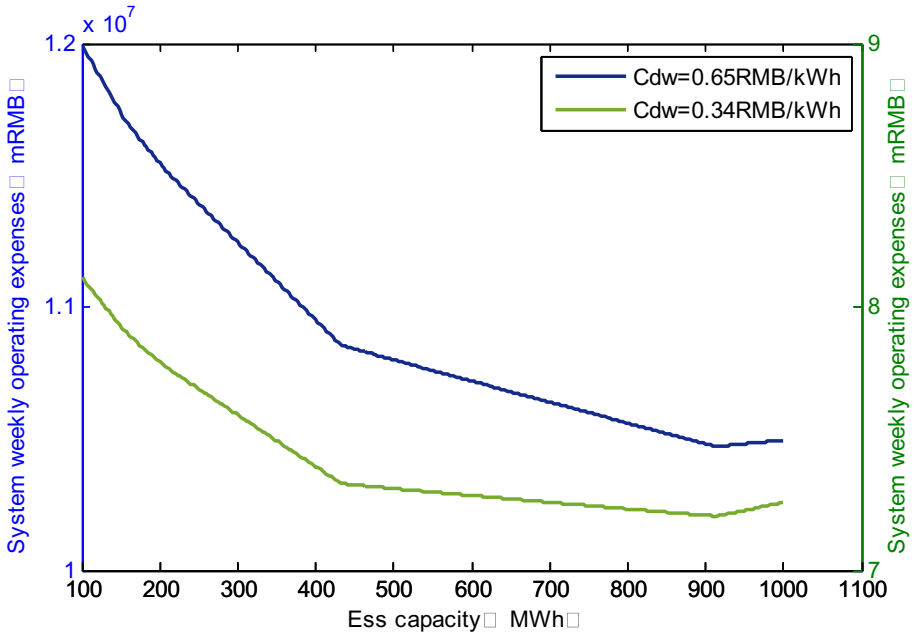

Fig. 16. Optimal ESS capacity corresponding to Cdw values of 0.34 RMB/KWh and 0.65 RMB/KWh.

that a change in the discarded electricity price at this stage has little effect on the optimal energy storage capacity. According to the system's operational mode described above in Section 2, the existing power market and retailer may have the possibility of acquiring discarded wind power at a low cost. Therefore, when the unit price of the discarded wind power and the unit price of the auxiliary peaking service differ, the changes in optimal energy storage capacity is simulated, with the results presented in Fig. 17.

It can observe that with a decrease of C_{dw} and C_{plo}, the optimal capacity of the ESS generally stepped down accordingly. This occurs because as the capacity of the ESS increases, the wind output range that can be satisfied above the reference load gradually increases. As the energy storage capacity continues to increase, the optimized wind output does not change, meaning that when the energy storage capacity reaches a certain high threshold value, the wind energy that cannot be absorbed by the ESS has only a few intervals that cause large differences in wind power output. If the capacity of the ESS continues to increase, the effect is very limited to the point of being negligible.

Only when the two unit prices increase sufficiently can the operating costs, which are brought about by the wasted energy that cannot be absorbed by the ESS within these intervals, possibly be further reduced through the increase of ESS capacity. Therefore, if C_{dw} and C_{plo} are sufficiently increased, the optimal ESS capacity also increases until the next large wind power difference can be fully processed. This then results in a large increase in capacity, which in turn causes a rapid increase in the optimal capacity of the ESS as C_{dw} and C_{plo} continue to increase. Conversely, if C_{dw} and C_{plo} are not large enough, it is of little significance to continue to increase energy storage capacity. Therefore, the optimal capacity of the ESS

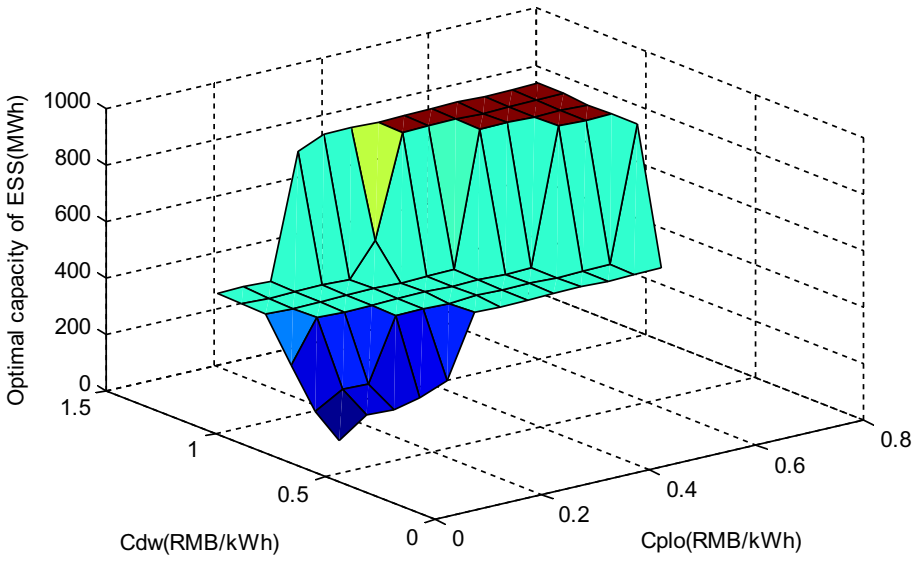

Fig. 17. Optimal capacity values of the ESS given different C_{dw} and C_{plo}.

Table 5
Four distinct scenarios in which Cdw and Cplo take on different values.

	C_{dw}	C_{plo}
The values in scenario one	0.34	1
The values in scenario two	0.34	0.5
The values in scenario three	0.1	1
The values in scenario four	0.1	0.5

Table 6
Comparison of optimal operating costs for the four methods used in this study.

	DPA	DPB	GA	RB
The cost in scenario one (mRMB/week)	7.066	7.291	7.208	7.492
The cost in scenario two (mRMB/week)	6.085	6.194	6.154	6.280
The cost in scenario three (mRMB/week)	4.360	4.562	4.492	4.763
The cost in scenario four (mRMB/week)	3.144	3.232	3.166	3.148

increases slowly as C_{dw} and C_{plo} continue to increase.

By determining the optimal energy storage capacity of the four methods when C_{dw} and C_{plo} are differ, we identify four distinct scenarios when C_{dw} and C_{plo} take on different values; we summarize these four scenarios in Table 5. Simulating these four different scenarios, we obtain the minimum operating costs of the system and compare these results, as seen in Table 6.

From the tables, it can observe that the higher values of C_{dw} and C_{plo}, the more operational profits are saved, indicating that the higher values of C_{dw} and C_{plo}, the more effective of the ESS is within the wind power plant. Compared with the GA method, the DPA method is able to save from 0.700% to 2.939% of operating costs; similarly, compared with the rules-based method, the DPA method is able to save from 0.127% to 8.461% of operating costs.

6. Conclusions

In this paper, a component sizing method for Wind-ESS system based on dynamic programming is proposed. By calculating both the penalty power under different ESS capacity and the operating costs of the corresponding BESS, it can be able to obtain an optimal ESS capacity. Our simulation results show the following key results.

(1) By comparing the effects that different algorithms have on the degradation of an ESS, it showed that the energy storage optimization configuration method based on multi-objective dynamic programming can effectively extend the lifespan of the ESS and obtain the optimal energy storage capacity.
(2) It also showed that the energy storage capacity we obtained from (1) has a positive impact on reducing the amount of wind power that is discarded by a wind power plant, thereby effectively reducing the operating costs of the given wind power plant.
(3) By changing both the unit price of the discarded wind energy and the unit price of the auxiliary peaking service, the change in operating costs of the system and the change of optimal capacity of the ESS is compared. It showed that the optimal capacity of the ESS decreased stepwise as the two unit prices decreased. This paper also determined that a change in the unit price of the recent discarded wind energy causes discarded wind power to have little effect on the optimal capacity of the ESS.

Overall, the proposed method was shown to effectively consider variations of output of a wind power plant and battery degradation caused by the irregular charging and discharging of the BESS. A reasonable ESS capacity configuration scheme can be achieved by our proposed method. In future work, to obtain a reasonable capacity allocation scheme, we will take into account the characteristics of different energy storage components, through the analysis of the function of different energy storage components in the new energy system. Meanwhile, we will build a small test platform to verify the method proposed in this paper.

Acknowledgements

This work was supported by the Science and Technology Foundation of State Grid Corporation of China Grant numbers: 52010119002F.

References

[1] H. Zhao, Q. Wu, S. Hu, et al., Review of energy storage system for wind power integration support, Appl. Energy 137 (2015) 545–553.
[2] A.M. Foley, P.G. Leahy, A. Marvuglia, et al., Current methods and advances in forecasting of wind power generation, Renew. Energy 37 (2012) 1–8.
[3] Zizhi Xu, Ming Zeng, Analysis on electricity market development in US and its inspiration to electricity market construction in China, Power Syst. Technol. 6 (2011) 161–166.
[4] F.J. Heredia, M.D. Cuadrado, C. Corchero, On optimal participation in the electricity markets of wind power plants with battery energy storage systems, Comput. Oper. Res. 96 (2018) 316–329.
[5] C.A. Sepulveda Rangel, L. Canha, M. Sperandio, et al., Methodology for ESS-type selection and optimal energy management in distribution system with DG considering reverse flow limitations and cost penalties, IET Gener., Transm. Distrib. 12 (2018) 1164–1170.
[6] N. Li, C. Uçkun, E.M. Constantinescu, et al., Flexible operation of batteries in power system scheduling with renewable energy, IIEEE Trans. Sustain. Energy 7 (2016) 685–696.
[7] P. Zou, Q. Chen, Q. Xia, et al., Evaluating the contribution of energy storages to support large-scale renewable generation in joint energy and ancillary service markets, IIEEE Trans. Sustain. Energy 7 (2016) 808–818.
[8] X. Ke, N. Lu, C. Jin, Control and size energy storage systems for managing energy imbalance of variable generation resources, IIEEE Trans. Sustain. Energy 6 (2017) 70–78.
[9] P. Xiong, C. Singh, Optimal planning of storage in power systems integrated with wind power generation, IIEEE Trans. Sustain. Energy 7 (2016) 232–240.
[10] F. Zhang, Z. Xu, K. Meng, Optimal sizing of substation-scale energy storage station considering seasonal variations in wind energy, IET Gener., Transm. Distrib. 10 (2016) 3241–3250.
[11] F. Zhang, G. Wang, K. Meng, et al., Improved cycle control and sizing scheme for wind energy storage system based on multi objective optimization, IIEEE Trans. Sustain. Energy 8 (2017) 966–977.
[12] F. Luo, K. Meng, Z.Y. Dong, et al., Coordinated operational planning for wind farm with battery energy storage system, IIEEE Trans. Sustain. Energy 6 (2015) 253–262.
[13] H. Bludszuweit, J.A. Dominguez-Navarro, A probabilistic method for energy storage sizing based on wind power forecast uncertainty, IEEE Trans. Power Syst. 26 (2011) 1651–1658.
[14] G. Hug, A. Kargarian, Optimal sizing of energy storage systems: a combination of hourly and intra-hour time perspectives, IET Gener., Transm. Distrib. 10 (2016) 594–600.
[15] K. Baker, G. Hug, X. Li, Energy storage sizing taking into account forecast uncertainties and receding horizon operation, IEEE Trans. Sustain. Energy 8 (2017) 331–340.
[16] Minglei Bao, Yi Ding, Changzheng Shao, et al., Review of nordic electricity market and its suggestions for China, Proc. CSEE 37 (2017) 4881–4898.
[17] B. Diouf, R. Pode, Potential of lithium-ion batteries in renewable energy, Renew. Energy 76 (2015) 375–380.
[18] B. Burgholzer, H. Auer, Cost/benefit analysis of transmission grid expansion to enable further integration of renewable electricity generation in Austria, Renew. Energy 97 (2016) 189–196.
[19] X. Han, M. Ouyang, L. Lu, et al., A comparative study of commercial lithium ion battery cycle life in electrical vehicle: aging mechanism identification, J. Power Sources 251 (2014) 38–54.
[20] X. Jin, C. Liu, Physics-based control-oriented reduced-order degradation model for LiNiMnCoO2 - graphite cell, Electrochim. Acta 312 (2019) 188–201.
[21] J. Wang, P. Liu, J. Hicks-Garner, et al., Cycle-life model for graphite-$LiFePO_4$ cells, J. Power Sources 196 (2011) 3942–3948.
[22] Z. Song, J. Li, X. Han, et al., Multi-objective optimization of a semi-active battery/supercapacitor energy storage system for electric vehicles, Appl. Energy 135 (2014) 212–224.
[23] Zifa Liu, Hanxiao Yu, Shuai Wang, et al., Transmission grid planning considering operation efficiency and wind curtailment loss, Power Syst. Technol. 42 (2018) 827–834.
[24] Outlook and application analysis of energy storage in power system with high renewable energy penetration, IOP Conf. Ser. Earth Environ. Sci. 121 (2018)

52–64.
[25] S. Wang, N. Zhang, L. Wu, et al., Wind speed forecasting based on the hybrid ensemble empirical mode decomposition and GA-BP neural network method, Renew. Energy 94 (2016) 629–636.
[26] J. Wu, X. Xing, X. Liu, et al., Energy management strategy for grid-tied microgrids considering the energy storage efficiency, IEEE Trans. Ind. Electron. 65 (12) (2018) 9539–9549.
[27] G. Xu, H. Cheng, S. Fang, et al., Optimal size and location of battery energy storage systems for reducing the wind power curtailments, Electr. Power Compon. Syst. 46 (2018) 1–11.
[28] G. Wang, M. Ciobotaru, V.G. Agelidis, Power smoothing of large solar PV plant using hybrid energy storage, IEEE Trans. Sustain. Energy 5 (2014) 834–842.
[29] G. Li, G. Weiss, M. Mueller, et al., Wave energy converter control by wave prediction and dynamic programming, Renew. Energy 48 (2012) 392–403.
[30] M. Khalid, A. Ahmadi, A.V. Savkin, et al., Minimizing the energy cost for microgrids integrated with renewable energy resources and conventional generation using controlled battery energy storage, Renew. Energy 97 (2016) 646–655.
[31] S. Zhang, R. Xiong, Adaptive energy management of a plug-in hybrid electric vehicle based on driving pattern recognition and dynamic programming, Appl. Energy 155 (2015) 68–78.
[32] A.N. Tu, M.L. Crow, A.C. Elmore, Optimal sizing of a vanadium redox battery system for microgrid systems, IEEE Trans. Sustain. Energy 6 (2017) 729–737.
[33] C.T. Li, Control and Optimization of Future Electric Grid Integrating Plug-In Electric Vehicles and Wind Power, the University of Michigan, 2013, pp. 48–50.
[34] W. Li, Framework of probabilistic power system planning, CSEE J. Power Energy Syst. 1 (2015) 1–8.
[35] W. Du, J. Bi, T. Wang, et al., Impact of grid connection of large-scale wind farms on power system small-signal angular stability, CSEE J. Power Energy Syst. 1 (2015) 83–89.
[36] Jianmin Duan, Zhixin Wang, Chengmin Wang, et al., Renewable power planning considering carbon emission reduction benefits, Power Syst. Technol. 39 (2015) 11–15.
[37] General Electric Company, White Paper: 2025 China Wind Power and Electricity Cost, vol 10, 2016.
[38] Haisheng Hong, Quanyuan Jiang, Yuting Yan, et al., An optimization control method of battery energy storage system with wind power fluctuations smoothed in real time, Autom. Electr. Power Syst. 37 (2013) 103–109.